Inorg. Chem. **2005**, *44*, 5222–5228

Anion-Controlled Nuclearity in Nickel Complexes with Potentially Dinucleating, Poly(oxime) Amine Ligands

Elizabeth A. Deters, Michael J. Goldcamp,[†] Jeanette A. Krause Bauer, and Michael J. Baldwin*

Department of Chemistry, University of Cincinnati, Cincinnati, Ohio 45221-0172

Received November 19, 2004

Two new ligands consisting of bis(oxime) amine units tethered by a bridge have been synthesized. Their nickel chloride and nickel nitrate complexes have also been synthesized and characterized by X-ray crystallography, FTIR, mass spectrometry, and elemental analysis. One of these ligands, **L1** (*N*,*N*′,*N*′,*N*′-tetra(1-propan-2-onyl oxime)-diamino-*m*-xylene), is always dinucleating, while the other ligand, **L2** (*N*,*N*,*N*′,*N*′-tetra(1-propan-2-onyl-oxime)-1,3-diaminopropane), shows an unusual anion dependence on the nuclearity. When nickel chloride is used, the ligand acts in a dinucleating manner and coordinates two nickels; however, when nickel nitrate is used, the ligand acts in a monodentate fashion and coordinates only one nickel. Once the mononuclear complex is formed, it is not possible to add a second nickel if $Ni(NO_3)_2$ is used as the nickel source; it is possible, however, to add a second nickel if $NiCl_2$ is used as the nickel source. The dinuclear complex can be converted to the mononuclear one by either using silver nitrate to exchange the chloride anions for nitrates or by dissolving the complex in water. Ni_2(**L1**)$Cl_4(DMF)_2$.DMF: orthorhombic, $P2_12_12_1$, $a = 12.2524(11)$ Å, $b = 16.6145(15)$ Å, $c = 20.1234(19)$ Å, $V = 4096.5(6)$ Å^3, $Z = 4$. [Ni_2(**L2**)Cl_4(DMF)]$_2$·2DMF: triclinic, P-1, $a = 12.5347(5)$ Å, $b = 12.5403(5)$ Å, $c = 14.3504(6)$ Å, $\alpha = 67.348(1)°$, $\beta = 69.705(1)°$, $\gamma = 81.549(1)°$, $V = 1952.25(14)$ Å^3, $Z = 1$. Ni(**L2**)·$(NO_3)_2$: monoclinic, $P2_1/n$, $a = 9.6738(3)$ Å, $b = 30.2229(9)$ Å, $c = 15.8238(5)$ Å, $\beta = 97.995(1)°$, $V = 4581.4(2)$ Å^3, $Z = 8$.

Introduction

The development of new ligands with less commonly used functional groups contributes to the discovery of new transition-metal catalysts and expands our understanding of the coordination chemistry of these groups in the context of polydentate ligands. The new polydentate ligands may also support biomimetic functions by their metal complexes, which can lend insight into metal-dependent biomolecules. The choice of mononucleating versus dinucleating ligands to control the nuclearity of the complex is important, as the nuclearity of catalysts and metalloenzyme active sites often determines their reactivity. Several examples of enzyme models show a nuclearity dependence on their catalytic activity. Often, the mononuclear complexes show either decreased or no activity compared to their dinuclear counterparts.[1−4] The ability to convert between an inactive mononuclear and active dinuclear species may lead to catalysts that can be turned on or off as needed.

Predictable nuclearity also is important in the design of larger, supramolecular structures, such as cyclophanes, triangles, and squares.[5−8] Understanding the factors that may be exploited to control nuclearity will add insight into how supramolecular structures assemble and will provide new routes for their construction. Indeed, several examples of anion-controlled assembly of supramolecular structures have been demonstrated.[9−14] Nickel amidinothiourea cage com-

* E-mail: Michael.Baldwin@uc.edu.
[†] Present location: Wilmington College, Wilmington, OH.

(1) Sarmah, S.; Kalita, D.; Hazarika, P.; Borah, R.; Islam, N. S. *Polyhedron* **2004**, *23*, 1097−1107.
(2) Parimala, S.; Kandaswamy, M. *Inorg. Chem. Commun.* **2003**, *6*, 1252−1254.
(3) Iranzo, O.; Elmer, T.; Richard, J. P.; Morrow, J. R. *Inorg. Chem.* **2003**, *42*, 7737−7746.
(4) Gajda, T.; Jancso, A.; Mikkola, S.; Lönnberg, H.; Sirges, H. *J. Chem. Soc., Dalton Trans.* **2002**, 1757−1763.
(5) Izatt, R. M.; Pawlak, K.; Bradshaw, J. S.; Bruening, R. L. *Chem. Rev.* **1995**, *95*, 2529−2586.
(6) Kryschenko, Y. K.; Seidel, R. S.; Arif, A. M.; Stang, P. J. *J. Am. Chem. Soc.* **2003**, *125* (17), 5193−5198.
(7) Nguyen, S. T.; Gin, D. L.; Hupp, J. T.; Zhang, X. *Proc. Nat. Acad. Sci. U.S.A.* **2001**, *98* (21), 11849−11850.
(8) Sun, S.; Stern, C. L.; Nguyen, S. T.; Hupp, J. T. *J. Am. Chem. Soc.* **2004**, *126*, 6314−6326.
(9) Vilar, R.; Mingos, D. M. P.; White, A. J. P.; Williams, D. J. *Angew. Chem., Int. Ed.* **1998**, *37* (9), 1258−1261.
(10) Harding, L. P.; Jeffery, J. C.; Riis-Johannessen, T.; Rice, C. R.; Zeng, Z. *J. Chem. Soc., Dalton Trans.* **2004**, *16*, 2396−2397.
(11) Harding, L. P.; Jeffery, J. C.; Riis-Johannessen, T.; Rice, C.; Zeng, Z. *Chem. Commun.* **2004**, *6*, 654−655.

10.1021/ic048355x CCC: $30.25
Published on Web 06/24/2005

Scheme 1. Poly(oxime), Dinucleating Ligands, **1** and **2**

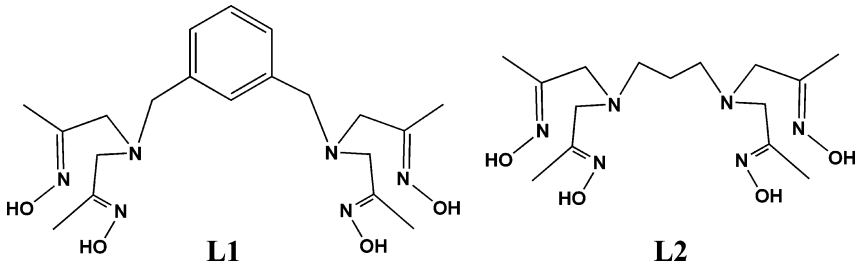

plexes have been constructed which differ in shape and formation on the basis of the anion used.[9] Different cobalt helical arrays have been built on the basis solely of anion choice.[10−11] There are copper-arginine supramolecular assemblies whose structure depends on the anion involved.[12] Anion control has also been used to direct the synthesis of silver supramolecular assemblies.[13−14] Thus, the work reported here on anion control of nuclearity adds to the arsenal of known, anion-controlled techniques for implementing the design of new supramolecular assemblies.

A series of dinucleating, poly(oxime) amine ligands consisting of two bis(oxime) amine motifs connected by a bridge from among those commonly used in dinucleating ligands[15−19] has been synthesized. These ligands were originally designed to complement the mononucleating ligands previously reported by Goldcamp et al.[20] to probe the effect of nuclearity on the oxygen reactivity of poly(oxime) nickel complexes. During the synthesis of these complexes, an unexpected anion effect on nuclearity was discovered. The ligand **L1**, *N*,*N*,*N*′,*N*′-tetra(propan-2-onyl oxime)-diamino-*m*-xylene (Scheme 1), predictably supports a dinuclear complex of Ni(II), regardless of the Ni(II) salt used. However, for Ni(II) complexes of **L2**, *N*,*N*,*N*′,*N*′-tetra-(1-propan-2-onyl oxime)-1,3-diamino propane (Scheme 1), a dependence of nuclearity on the anion is seen. When $NiCl_2$ is reacted with **L2**, it coordinates two nickels, providing a tridentate motif for each; however, when $Ni(NO_3)_2$ is used, it acts in a hexadentate manner and coordinates one nickel. Thus, the nuclearity of **L2** can be controlled by varying the nickel salt used. This Paper explores the structures and interconversion of the mononuclear and dinuclear complexes of **L2**, compares them to complexes of **L1**, and determines whether the anion control is a kinetic or thermodynamic effect.

(12) Ohata, N.; Masuda, H.; Yamauchi, O. *Inorg. Chim. Acta* **2000**, *300*−*302*, 749−761.
(13) Schultheiss, N.; Powell, D. R.; Bosch, E. *Inorg. Chem.* **2003**, *42*, 8886−8890.
(14) Sailaja, S.; Rajasekharan, M. V. *Inorg. Chem.* **2003**, *42*, 5675−5684.
(15) Ghosh, D.; Mukherjee, R. *Inorg. Chem.* **1998**, *37*, 6597−6605.
(16) Barrios, A. M.; Lippard, S. J. *Inorg. Chem.* **2001**, *40* (5), 1060−1064.
(17) Itoh, S.; Bandoh, H.; Nakagawa, M.; Nagatomo, S.; Kitagawa, T.; Karlin, K. D.; Fukuzumi, S. *J. Am. Chem. Soc.* **2001**, *123*, 11168−11178.
(18) Sakiyama, H.; Igarashi, T.; Nakayama, Y.; Hossain, M. K.; Unoura, K.; Nashida, Y. *Inorg. Chim. Acta* **2003**, *351*, 256−260.
(19) Liang, H.; Henson, M. J.; Hatcher, L. Q.; Vance, M. A.; Zhang, C. X.; Lahti, D.; Kaderli, S.; Sommer, R. D.; Rheingold, A. L.; Zuberbuehler, A. D.; Solomon, E. I.; Karlin, K. D. *Inorg. Chem.* **2004**, *43* (14), 4115−4117.
(20) Goldcamp, M. J.; Edison, S. E.; Squires, L. N.; Rosa, D. T.; Vowels, N. K.; Coker, N. L.; Krause Bauer, J. A.; Baldwin, M. J. *Inorg. Chem.* **2003**, *42*, 717−728.

Experimental Section

Syntheses. All chemicals were obtained from Fisher or Aldrich and were used without further purification unless otherwise noted. The alkylating reagent *N*,*N*,*N*-triethyl-*N*-(propan-2-onyl oxime)-ammonium chloride, TACO, was prepared as previously reported.[21]

***N*,*N*,*N*′,*N*′-Tetra(propan-2-onyl oxime)-diamino-*m*-xylene (L1).** In a 250-mL round-bottom flask, 0.70 mL (8.1 mmol) of *m*-xylylenediamine was suspended in 150 mL of *i*-propanol. To this solution, 6.20 g (29.7 mmol) of TACO was added. The suspension was heated to reflux and stirred for 2 h. After cooling to room temperature, the solvent was removed by rotary evaporation, yielding an orange oil. The product was removed from the oil by extraction of impurities with acetone and the resulting brown solid was purified by suspension in boiling water. The result was a slightly tan powder, 1.10 g (60% yield).

^{1}H NMR, ppm (in d_6-DMSO): 10.6s, 7.2m, 3.4s, 2.9s, 1.7s; IR, cm^{-1}: 2925w, 2823w, 2361w, 1636w, 1427m, 1258w, 1119w, 1026s, 932s, 733m, 509w; mass spec. (TOF MS ES+), 421.3 (M^+); d.p.= 160−160.5 °C.

Ni_2(L1)Cl_4. A solution of 0.78 g (3.3 mmol) of $NiCl_2{\cdot}6H_2O$ dissolved in 10 mL of methanol was added to a solution of 0.56 g (1.3 mmol) of **L1** dissolved in 20 mL of methanol over a period of 5 min. The resulting blue solution was stirred for 4 h. The solvent was removed via rotary evaporation, and the product was removed from the excess $NiCl_2$ by extraction with acetonitrile, which was removed via rotary evaporation. The product was a greenish-blue solid, 0.85 g (96% yield). Crystals suitable for X-ray crystallography were obtained by vapor diffusion of diethyl ether into a DMF solution of Ni_2(**L1**)Cl_4.

IR, cm^{-1}: 2366w, 1623s, 1468m, 1435s, 1369w, 1315w, 1294w, 1234s, 1159m, 1098w, 1066s, 1015m, 937m, 859m, 816w, 748w, 724w, 671w, 602w, 522w; mass spec. (TOF MS ES+): 533 (M^+ − 2Cl); Elemental analysis for $Ni_2C_{20}H_{32}N_6O_4Cl_4$: found, C 37.83%, H 5.72%, N 13.46%; calcd, C 37.81%, H 5.61%, N 13.57%.

Ni_2(L1)$(NO_3)_4$. In a 50-mL Erlenmeyer flask, 0.10 g (0.24 mmol) of **L1** was dissolved in 20 mL of methanol. To this solution, 0.16 g (0.55 mmol) of $Ni(NO_3)_2{\cdot}6H_2O$ dissolved in 10 mL of methanol was added over 5 min. The blue solution was stirred for 4 h, during which time the product precipitated out of solution. The product, a light blue solid, was isolated by filtration, 0.22 g (98% yield).

IR, cm^{-1}: 2384w, 1764w, 1637m, 1498m, 1381s, 1231m, 1163w, 1065s, 1018m, 931m, 908w, 847w, 807m, 729w, 683m, 603w, 515w; mass spec. (TOF MS ES+): 846.06 (M^+ + formate, added to the sample to facilitate ionization); elemental analysis for $Ni_2C_{20}H_{32}N_6O_4(NO_3)_4{\cdot}H_2O$: found, C 29.84%, H 4.28%, N 17.17%; calcd, C 29.88%, H 4.26%, N 17.42%.

***N*,*N*,*N*′,*N*′-Tetra(1-propan-2-onyl oxime)-1,3-diaminopropane (L2).** In a 250-mL round-bottom flask, 1.0 mL (12 mmol) of

(21) Goldcamp, M. J.; Rosa, D. T.; Landers, N. A.; Mandel, S. M.; Krause Bauer, J. A.; Baldwin, M. J. *Synthesis* **2000**, *14*, 2033−2038.

1,3-diaminopropane was suspended in 150 mL of *i*-propanol. To this suspension, 13.86 g (66.40 mmol) of TACO was added. The suspension was heated to reflux and stirred for 2.5 h. After cooling, the solvent was removed via rotary evaporation, giving an orange oil. Impurities were removed from the product by suspension of the oil in diethyl ether, which causes precipitation of most impurities. After filtration, the ether was removed by rotary evaporation and the resulting orange oil was dissolved in the minimum amount of ethyl acetate and run through a 20-cm silica gel column, using 90/10 ethyl acetate/ethanol as eluent. The colorless and pale yellow fractions were combined and the solvent was removed. The product was dried under high vacuum for 24 h, giving an off-white solid, 1.9 g (44% yield). Note: This compound is extremely hydroscopic and will return to an oil if exposed to ambient atmosphere for more than ~20 min. It can be resolidified by putting the oil under vacuum again.

^{1}H NMR, ppm (d_6-DMSO):10.5s, 2.9s, 2.2t, 1.9m, 1.5s; IR, cm^{-1}: 2940m, 2747m, 2662s, 2492m, 2268w, 2031w, 1623w, 1466s, 1394s, 1165m, 1036s, 954w, 807w; mass spec. (TOF MS ES+) 359 (M^+). The hydroscopic nature of this compound prevents an accurate melting point determination.

Ni_2(L2)Cl_4. To a solution of 0.48 g (1.3 mmol) of **L2** dissolved in 20 mL of methanol, a solution of 0.76 g (3.2 mmol) of $NiCl_2 \cdot 6H_2O$ in 10 mL of methanol was added over 5 min. The blue solution was stirred for 24 h, and the methanol was removed by rotary evaporation. The product was extracted from the excess $NiCl_2$ with acetonitrile, which was removed via rotary evaporation. The final product was a light green solid, 0.76 g (94% yield). X-ray quality crystals were obtained by vapor diffusion of diethyl ether into a DMF solution of Ni_2(**L2**)Cl_4.

IR, cm^{-1}: 2373w, 1627s, 1445s, 1410s, 1377s, 1292m, 1239s, 1136m, 1069s, 1033w, 999w, 940m, 853m, 760w, 671w; mass spec (TOF MS ES+): 545 ($M^+ - 4Cl$); elemental analysis for $Ni_2C_{15}H_{31}N_6O_4Cl_4(DMF)_2$: found, C 32.90%, H 6.22%, N14.59%; calcd, C 33.02%, H 5.81%, N 14.67%.

Ni(L2)·$(NO_3)_2$. A 10-mL solution of 0.41 g (1.4 mmol) of $Ni(NO_3)_2 \cdot 6H_2O$ in methanol was added to a 10-mL solution of 0.53 g (1.4 mmol) of **L2** in methanol. The resulting solution was stirred at ambient temperature overnight, and the product was recovered by evaporation of the solvent to give a pink powder, 0.57 g (96% yield). Crystals suitable for X-ray crystallography were obtained by vapor diffusion of diethyl ether into a DMF solution of Ni(**L2**)·$(NO_3)_2$.

IR, cm^{-1}: 2320w, 1673s, 1466s, 1373s, 1285s, 1151w, 1123m, 1091w, 1030s, 927m, 892m, 854w, 825m, 717w, 672m, 649w, 549w, 512w, 474w; mass spec (TOF MS ES+): 417 (M^+); elemental analysis for $Ni_1C_{15}H_{31}N_6O_4 \cdot (NO_3)_2$: found, C 33.39%, H 5.49%, N 20.61%; calcd, C 33.29%, H 5.59%, N 20.71%.

Reactivity. Ni(L2)·$(NO_3)_2$ + $Ni(NO_3)_2$. 0.50 g of Ni(**L2**)·$(NO_3)_2$ (1.1 mmol) was dissolved in 50 mL of methanol. 0.80 g (2.8 mmol) of $Ni(NO_3)_2 \cdot 6H_2O$, 2.5 equivalents, was added to the solution, which was stirred for 1.5 days at reflux. A UV−visible spectrum of the resulting solution was then obtained.

Ni(L2)·$(NO_3)_2$ + $NiCl_2$ in Methanol. 0.10 g of Ni(**L2**)·$(NO_3)_2$ (0.25 mmol) was dissolved in 25 mL of methanol. 0.22 g (0.8 mmol)of $NiCl_2 \cdot 6H_2O$, 3.8 equivalents, was added to the solution, which was stirred for 30 h at reflux. During this time, a green precipitate formed. After isolation of the solid by filtration, an IR spectrum of the solid was obtained.

Ni(L2)·$(NO_3)_2$ + $NiCl_2$ in Water. 0.10 g of Ni(**L2**)·$(NO_3)_2$ (0.25 mmol) was dissolved in 10 mL of water. 0.23 g (0.98 mmol) of $NiCl_2 \cdot 6H_2O$, 3.9 equivalents, was added to the solution. The resulting solution was stirred for 21 h at room temperature, after which time a UV−visible spectrum of the reaction solution was taken.

Ni_2(L2)Cl_4 + $AgNO_3$. Ni_2(**L2**)Cl_4, 0.36 g (0.59 mmol), was dissolved in 10 mL of water. To this solution, 0.40 g (2.3 mmol) of solid silver nitrate was added, resulting in the almost immediate precipitation of silver chloride. The solution was stirred at room temperature for 20 h. The silver chloride was filtered from the solution, leaving a pink colored solution. The resulting nickel complex was separated from the excess nickel by precipitation from acetone.

Ni_2(L2)Cl_4 in Water. Ni_2(**L2**)Cl_4, 0.14 g (0.23 mmol), was dissolved in 15 mL of deionized water. Spectra of the solution were taken every 20 s for 40 min and then every 1 min for 1 h.

Ni_2(L1)Cl_4 in Water. A solution of 0.15 g of Ni_2(**L1**)Cl_4 (0.22 mmol) was dissolved in 15 mL of deionized water. UV−visible absorption spectra were acquired every minute for 2 h and then every 30 min for 16 h.

Physical Methods. NMR spectra were collected on a Bruker AC250 250 MHz narrow bore, broad-band spectrometer. IR spectra were collected from solid samples dispersed in KBr pellets on a BioRad Excalibur Series FTIR spectrophotometer. Melting points were taken on a MelTemp instrument from Laroratory Instruments. The UV−visible absorption spectra were taken with a Spectral Instruments model 430 fiber optic dip probe spectrophotometer or a Perkin-Elmer model λ40 spectrophotometer. Mass spectra were obtained using a Micromass Q-TOF-II instrument. Elemental analysis was performed by Quantitative Technologies Inc (Whitehouse, NJ).

X-ray Crystallography. Intensity data were collected at 150 K on a Bruker SMART6000 CCD diffractometer (Mo Kα radiation and graphite monochromator, $\lambda = 0.71073$ Å) and were processed using the Bruker suite of programs.[22a] Intensities were corrected for Lorentz, polarization, and decay effects. Absorption and beam corrections based on the multiscan technique were applied using SADABS.[22b] The structures were solved using SHELXTL[22c] and were refined by full-matrix least squares on F^2. For all compounds, non-hydrogen atoms were refined with anisotropic displacement parameters. The O−H hydrogen atoms were located directly in the difference map and held fixed at that location. All remaining hydrogen atoms were either located or calculated and treated with a riding model in subsequent refinements. For $[Ni_2$(**L2**)$Cl_4(DMF)]_2$, the molecule crystallizes with two badly disordered DMF solvent molecules. A suitable refinement of these DMF molecules was not forthcoming. Therefore, the solvent contribution to the reflection data was removed using the program SQUEEZE.[22d] The crystallographic data are summarized in Table 1.

Results

Two new, poly(oxime) containing ligands, **L1** and **L2**, have been synthesized (Scheme 1). Each ligand consists of two bis(oxime) amine units tethered by a bridge. In the case

(22) (a) Bruker SMART v5.628 and SAINT v6.36A were used for data collection and processing, respectively; Bruker Analytical X-ray Instruments, Inc. Madison, WI. (b) SADABS v2.05 was used for the application of multiscan absorption and beam corrections, G. M. Sheldrick, University of Gõttingen, Germany. (c) SHELXTL v6.12 was used for the structure solution and generation of figures and tables, G. M. Sheldrick, University of Gõttingen, Germany and Bruker Analytical X-ray Instruments, Inc. Madison, WI. (d) Spek, A. L. Univerity of Utrecht, The Netherlands, 1992. SQUEEZE is a routine implemented in PLATON allowing solvent contributions to be eliminated from the reflection data.

Table 1. Crystallographic Data

	1 $Ni_2(L1)Cl_4(DMF)_2 \cdot DMF$	**2** $[Ni_2(L2)Cl_4(DMF)]_2 \cdot 2DMF$	**3** $Ni(L2)(NO_3)_2$
formula	$C_{26}H_{46}N_8O_6Cl_4Ni_2 \cdot C_3H_7NO$	$C_{36}H_{74}N_{14}O_{10}Cl_8Ni_4 \cdot 2(C_3H_7NO)$	$[C_{15}H_{30}N_6O_4Ni](NO_3)_2$
fw	899.02	1527.72	541.18
temperature, K	150(2)	150(2)	150(2)
crystal system	orthorhombic	triclinic	monoclinic
space group	$P2_12_12_1$	P-1	$P2_1/n$
a, Å	12.2524(11)	12.5347(5)	9.6738(3)
b, Å	16.6145(15)	12.5403(5)	30.2229(9)
c, Å	20.1234(19)	14.3504(6)	15.8238(5)
α,°	90	67.348(1)	90
β,°	90	69.705(1)	97.995(1)
γ,°	90	81.549(1)	90
volume, Å^3	4096.5(6)	1952.25(14)	4581.4(2)
Z	4	1	8
ρ_{calc}, Mg/m^3	1.458	1.299	1.569
reflns collected	55970	24188	55816
indep. reflns/ R_{int}	10221/0.0651	8585/0.0615	11384/0.0342
goodness-of-fit	1.005	0.891	1.010
R_1/wR_2 [$I > 2\sigma(I)$][a]	0.0334/0.0768	0.0480/0.1171	0.0286/0.0663
R_1/wR_2 (all data)[a]	0.0461/0.0811	0.0855/0.1292	0.0417/ 0.0731

[a] $R_1 = \sum|F_o| - |F_c|/\sum|F_o|$, $wR_2 = [\sum(F_o^2 - F_c^2)^2/\sum w(F_o^2)^2]^{1/2}$.

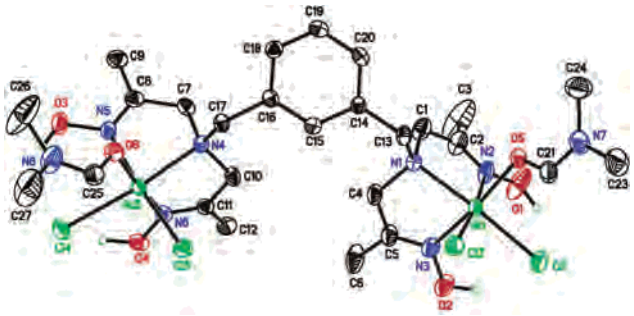

Figure 1. ORTEP diagram of Ni_2(**L1**)$Cl_4(DMF)_2$. H atoms are omitted for clarity, with the exception of hydroxyl groups.

of **L1**, the bridge is a rigid phenyl ring. For **L2**, the bridge is a more flexible *n*-propyl chain.

When nickel is coordinated to **L1**, regardless of the counteranion, a blue, dinuclear nickel complex results. The blue complex with $Ni(NO_3)_2$ is shown to be dinuclear by mass spectrometry and elemental analysis, but a crystal suitable for X-ray crystallography has not yet been obtained. The crystal structure of the chloride complex obtained from DMF is shown in Figure 1. Ni_2(**L1**)$Cl_4(DMF)_2$ crystallizes in the $P2_12_12_1$ space group. Each nickel is in a pseudo-octahedral environment, coordinated by two oxime nitrogens, one amine nitrogen, two chlorides, and a DMF molecule. Selected bond lengths and angles are listed in Table 2. The average distance between the nickel and an oxime nitrogen is 2.040 Å, while the average distance from the metal to an amine nitrogen is 2.158 Å. The nickel−chloride bonds have an average distance of 2.412 Å.

When nickel chloride is added to **L2**, a blue, dinuclear complex forms, as expected (Figure 2). In the solid state, two of the dinuclear units are linked by a pair of chloride bridges. Each nickel has a pseudo-octahedral coordination sphere comprised of two oxime nitrogens, an amine nitrogen, two chlorides, and a DMF molecule. Selected bond lengths and angles for this complex are listed in Table 3. The average nickel−nitrogen (oxime) distance is 2.048 Å; the average nickel−nitrogen (amine) distance is 2.173 Å. The average

Table 2. Selected Bond Lengths (Å) and Bond Angles (°) for Ni_2(**L1**)$Cl_4(DMF)_2$

Ni(1)−N(1)	2.165(2)	Ni(1)−N(2)	2.053(2)
Ni(1)−N(3)	2.039(2)	Ni(1)−Cl(1)	2.4511(8)
Ni(1)−Cl(2)	2.3595(7)	Ni(1)−O(5)	2.0435(19)
Ni(2)−N(4)	2.150(2)	Ni(2)−N(5)	2.036(2)
Ni(2)−N(6)	2.035(2)	Ni(2)−Cl(3)	2.3737(7)
Ni(2)−Cl(4)	2.4660(7)	Ni(2)−O(6)	2.0511(17)
O(1)−N(2)	1.399(3)	O(2)−N(3)	1.405(3)
O(4)−N(6)	1.400(3)	O(3)−N(5)	1.387(3)
(N1)−C(13)	1.500(3)	N(4)−C(17)	1.501(3)
N(2)−Ni(1)−N(1)	79.19(9)	N(3)−Ni(1)−N(1)	79.42(9)
N(3)−Ni(1)−N(2)	85.92(10)	Cl(2)−Ni(1)−Cl(1)	97.76(3)
N(3)−Ni(1)−O(5)	172.56(9)	N(1)−Ni(1)−Cl(1)	163.78(6)
O(1)−N(2)−Ni(1)	123.90(18)	O(2)−N(3)−Ni(1)	124.24(17)
N(5)−Ni(2)−N(4)	78.88(8)	N(6)−Ni(2)−N(4)	77.06(8)
N(6)−Ni(2)−N(5)	93.73(9)	Cl(3)−Ni(2)−Cl(4)	99.56(3)
N(6)−Ni(2)−O(6)	175.27(8)	N(4)−Ni(2)−Cl(4)	160.58(6)
O(3)−N(5)−Ni(2)	123.07(15)	O(4)−N(6)−Ni(2)	125.29(16)

distance between a nickel and a nonbridging chloride is 2.421 Å, while the bridging chloride distances are slightly shorter, with an average distance of 2.419 Å.

When nickel nitrate is added to **L2**, however, a pink, mononuclear complex is formed (Figure 3). The nickel resides in a pseudo-octahedral coordination environment. Unlike Ni_2(**L1**)$Cl_4(DMF)_2$ and $[Ni_2$(**L2**)$Cl_4(DMF)]_2$, there are no counteranions bound directly to the nickel, so the dication

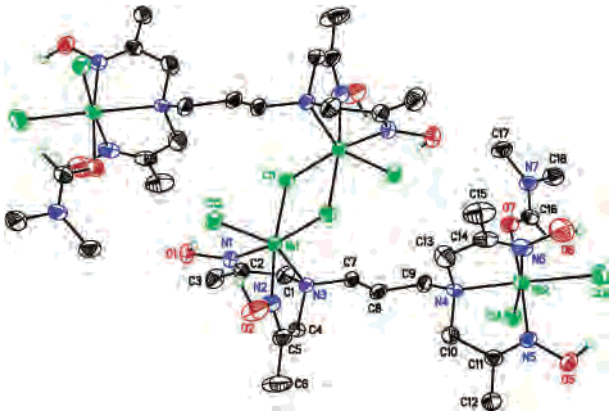

Figure 2. ORTEP diagram of $[Ni_2$(**L2**)$Cl_4(DMF)]_2$. H atoms are omitted for clarity, with the exception of hydroxyl groups.

Table 3. Selected Bond Lengths (Å) and Bond Angles (deg) for $[Ni_2(\mathbf{L2})Cl_4(DMF)]_2$

Ni(1)−N(1)	2.052(3)	Ni(1)−N(2)	2.032(3)
Ni(1)−N(3)	2.212(3)	Ni(1)−Cl(1)	2.4097(10)
Ni(1)−Cl(1A)	2.4284(10)	Ni(1)−Cl(2)	2.4732(10)
Ni(2)−N(4)	2.173(3)	Ni(2)−N(5)	2.052(3)
Ni(2)−N(6)	2.057(3)	Ni(2)−Cl(3)	2.4239(11)
Ni(2)−Cl(4)	2.3652(11)	Ni(2)−O(7)	2.079(3)
O(1)−N(1)	1.411(4)	O(2)−N(2)	1.397(4)
O(5)−N(5)	1.396(4)	O(6)−N(6)	1.396(4)
N(3)−C(7)	1.499(4)	N(4)−C(9)	1.488(5)
N(2)−Ni(1)−N(1)	93.78(13)	N(1)−Ni(1)−N(3)	75.59(12)
N(2)−Ni(1)−N(3)	77.84(12)	Cl(1)−Ni(1)−Cl(1A)[a]	83.44(3)
Cl(1A)[a]−Ni(1)−Cl(2)	90.03(4)	Cl(1)−Ni(1)−Cl(2)	100.51(4)
N(2)−Ni(1)−Cl(1)	172.45(9)	N(2)−Ni(1)−Cl(1A)[a]	94.37(10)
N(3)−Ni(1)−Cl(2)	155.95(8)	O(1)−N(1)−Ni(1)	123.3(2)
O(2)−N(2)−Ni(1)	123.2(2)	N(5)−Ni(2)−N(4)	80.14(12)
N(5)−Ni(2)−N(6)	88.02(13)	N(6)−Ni(2)−N(4)	78.38(13)
Cl(4)−Ni(2)−Cl(3)	96.93(4)	N(5)−Ni(2)−O(7)	173.10(12)
N(4)−Ni(2)−Cl(3)	164.21(9)	O(5)−N(5)−Ni(2)	126.0(2)
O(6)−N(6)−Ni(2)	124.2(3)		

[a] Symmetry operator = $-x + 1, -y, -z + 1$.

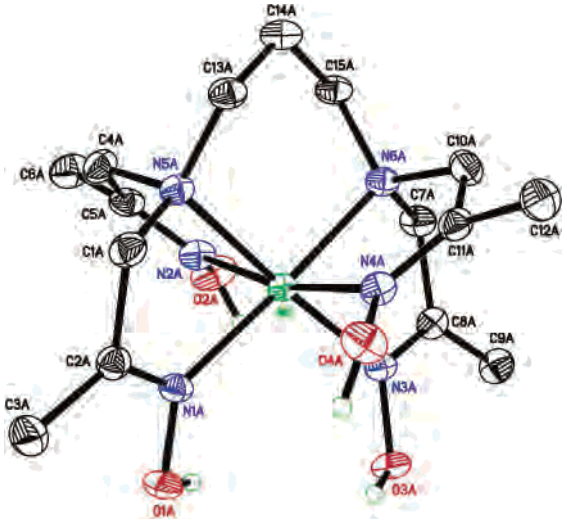

Figure 3. ORTEP diagram of Ni(**L2**)·$(NO_3)_2$. Only one independent molecule is shown. Anions and non-hydroxyl hydrogen atoms are omitted for clarity.

is coordinated only by the four oxime nitrogens and the two amine nitrogens on the ligand. Selected bond lengths and angles for this complex are listed in Table 4. The average nickel−nitrogen (oxime) distance is 2.074 Å and the average nickel−nitrogen (amine) distance is 2.098 Å. Because of the coordination mode, there is also an unusual C−C−C angle (mol. A: 120.88°; mol. B: 119.37°) in the propyl bridge of the ligand. The UV−visible spectra of all three compounds are shown in Figure S-1, Supporting Information.

Addition of excess nickel nitrate to Ni(**L2**)·$(NO_3)_2$ does not result in uptake of a second nickel, regardless of reaction time (up to 1.5 days) or temperature (up to reflux in methanol). The UV−visible spectra (Figure S-2, Supporting Information) show that the reaction solution contains nothing more than a combination of Ni(**L2**)·$(NO_3)_2$ and nickel nitrate. No dinuclear complex is formed. If $NiCl_2$ is used as the added nickel source, however, the mononuclear complex takes up a second nickel. With the addition of excess $NiCl_2$ to a methanol solution of Ni(**L2**)·$(NO_3)_2$, a green precipitate (consistent with a dinuclear complex) forms after several hours at reflux. An IR spectrum of this precipitate was

Table 4. Selected Bond Lengths (Å) and Bond Angles (deg) for Ni(**L2**)·$(NO_3)_2$

Ni(1)−N(1A)	2.0487(14)	Ni(1)−N(2A)	2.1146(14)
Ni(1)−Ni(3A)	2.0320(14)	Ni(1)−N(4A)	2.1012(13)
Ni(1)−N(5A)	2.1008(13)	Ni(1)−N(6A)	2.0938(14)
O(1A)−N(1A)	1.3976(17)	O(2A)−N(2A)	1.3956(18)
O(3A)−N(3A)	1.3978(17)	O(4A)−N(4A)	1.4039(17)
N(5A)−C(13A)	1.489(2)	N(6A)−C(15A)	1.487(2)
N(1A)−Ni(1)−N(5A)	78.71(5)	N(2A)−Ni(1)−N(1A)	88.99(5)
N(3A)−Ni(1)−N(1A)	104.75(5)	N(3A)−Ni(1)−N(4A)	89.03(5)
N(3A)−Ni(1)−N(6A)	79.40(5)	N(6A)−Ni(1)−N(5A)	97.17(5)
N(4A)−Ni(1)−N(6A)	80.28(5)	N(1A)−Ni(1)−N(6A)	175.48(5)
N(4A)−Ni(1)−N(2A)	167.74(5)	N(3A)−Ni(1)−N(5A)	176.36(5)
O(1A)−N(1A)−Ni(1)	128.70(10)	O(2A)−N(2A)−Ni(1)	129.78(11)
O(3A)−N(3A)−Ni(1)	128.14(10)	O(4A)−N(4A)−Ni(1)	128.32(10)
Ni(2)−N(1B)	2.0799(14)	Ni(2)−N(2B)	2.0979(13)
Ni(2)−N(3B)	2.0831(13)	Ni(2)−N(4B)	2.0496(14)
Ni(2)−N(5B)	2.1058(14)	Ni(2)−N(6B)	2.1014(13)
O(1B)−N(1B)	1.3974(17)	O(2B)−N(2B)	1.3968(17)
O(3B)−N(3B)	1.4008(16)	O(4B)−N(4B)	1.4102(17)
N(5B)−C(13B)	1.494(2)	N(6B)−C(15B)	1.495(2)
N(1B)−Ni(2)−N(5B)	79.59(5)	N(2B)−Ni(2)−N(1B)	85.51(5)
N(3B)−Ni(2)−N(1B)	106.90(5)	N(3B)−Ni(2)−N(4B)	87.54(5)
N(3B)−Ni(2)−N(6B)	78.54(5)	N(6B)−Ni(2)−N(5B)	95.01(5)
N(4B)−Ni(2)−N(6B)	79.95(5)	N(1B)−Ni(2)−N(6B)	174.48(5)
N(4B)−Ni(2)−N(2B)	171.42(5)	N(3B)−Ni(2)−N(5B)	173.18(5)
O(1B)−N(1B)−Ni(2)	129.33(10)	O(2B)−N(2B)−Ni(2)	130.28(10)
O(3B)−N(3B)−Ni(2)	130.69(10)	O(4B)−N(4B)−Ni(2)	125.89(10)

obtained, and comparison of the spectrum to a known sample of $Ni_2(\mathbf{L2})Cl_4$ shows the isolated solid to be the dinuclear complex (Figure S-3, Supporting Information). This phenomenon is not seen, however, when water is used as the solvent. Adding excess $NiCl_2$ to a solution of Ni(**L2**)·$(NO_3)_2$ in water does not result in the uptake of a second nickel, even after 21 h. The UV−visible spectrum of the reaction solution is nothing more than a combination of the mononuclear complex and $NiCl_2$ (Figure S-4, Supporting Information).

The dinuclear complex is easily converted into the mononuclear complex. Addition of $AgNO_3$ to an aqueous solution of $Ni_2(\mathbf{L2})Cl_4$ results in immediate precipitation of silver chloride as well as an almost instantaneous color change from the blue color of the dinuclear complex to the pink color of the mononuclear complex. After filtration of the silver chloride, a UV−visible spectrum, Figure 4, shows the reaction solution to contain a combination of the mononuclear

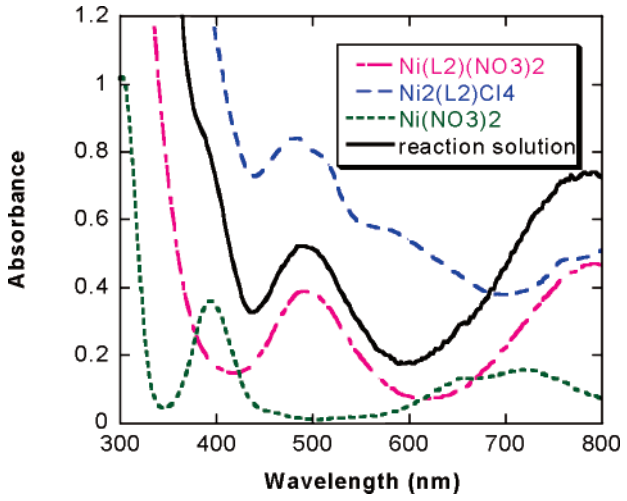

Figure 4. UV−visible spectra of nickel nitrate, Ni(**L2**)$(NO_3)_2$, $Ni_2(\mathbf{L2})Cl_4$, and reaction solution after reaction of the dinuclear complex with silver nitrate in water.

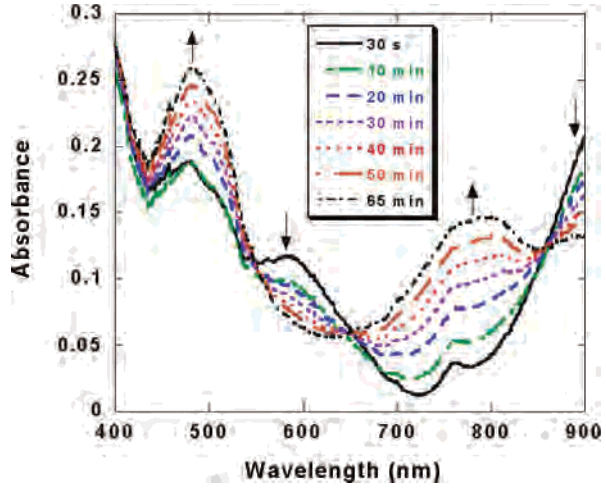

Figure 5. Change in UV−visible spectra of Ni_2(**L2**)Cl_4 in water over 1 h.

complex and nickel nitrate, with no remaining dinuclear complex. Thus, the exchange of the anion leads to a rapid change in nuclearity. On a longer time scale, the spontaneous conversion of the dinuclear complex to the mononuclear one is observed in aqueous solution. If Ni_2(**L2**)Cl_4 is dissolved in water, it will convert to the mononuclear species in about an hour, even without the addition of silver nitrate (Figure 5). The presence of three isosbestic points indicates that the dinuclear species converts to the mononuclear species without buildup of observable intermediates. This conversion is not seen if the complex is dissolved in methanol or acetonitrile. Conversion of the dinuclear complex to a mononuclear one is not seen in the complex with the phenyl-spaced ligand, Ni_2(**L1**)Cl_4, which remains dinuclear for at least 18 h when dissolved in water (Figure S-5, Supporting Information). A summary of the conditions in which the mononuclear and dinuclear complexes of **L2** are formed and interconvert are shown in Scheme 2.

Discussion

The dinuclear complexes in these studies show structural similarities to a series of mononuclear, bis(oxime) amine complexes.[20] The nickel−nitrogen (oxime) and nickel−nitrogen (amine) distances observed in the dinuclear complexes fall within the range of distances 1.992−2.099 Å and 2.085−2.207 Å, respectively, observed in the mononuclear bis(oxime) complexes. When the previous mononuclear, bis(oxime) complexes are made with nickel chloride, the solid-state structures are chloride-bridged dimers.[20] One notices the same phenomenon with Ni_2(**L2**)Cl_4, which also adopts a dimeric, chloride-bridged structure in the solid state (Figure 2). Ni_2(**L1**)Cl_4 (Figure 1) remains a dinuclear monomer in the solid state, as DMF molecules from the crystallization solvent coordinate in place of the bridging chloride from a second unit.

One striking difference between the Ni_2(**L1**)$Cl_4(DMF)_2$ and $[Ni_2$(**L2**)$Cl_4(DMF)_2]_2$ dinuclear complexes and the Ni(**L2**)·$(NO_3)_2$ mononuclear complex is the relative bond lengths for the Ni−N (amine) versus Ni−N (oxime) interactions. In the dinuclear complexes, the Ni−N (amine) distances are longer than the Ni−N (oxime) distances, whereas these distances are similar in the mononuclear complex. This difference can be attributed to a change in the Jahn−Teller axis of the d^8 ion. In the dinuclear complexes, the elongated axis encompasses the amine nitrogen and a chloride; thus, the Ni−N (amine) distances are significantly longer than the Ni−N (oxime) distances. However, in the mononuclear complex, the elongated axis lies along two oxime arms. The difference between the Ni−N (amine) and equatorial Ni−N (oxime) distances is, therefore, smaller in this complex.

The UV−visible spectra of Ni_2(**L1**)Cl_4, Ni_2(**L2**)Cl_4, and Ni(**L2**)·$(NO_3)_2$ are shown in Figure S-1, Supporting Information. There are three generally observed transitions for a d^8 ion in O_h symmetry: $^3A_{2g}(F)$ to $^3T_{2g}(F)$, $^3T_{1g}(F)$, or $^3T_{1g}(P)$.[23] For both Ni_2(**L1**)Cl_4 and Ni_2(**L2**)Cl_4, the transitions are assigned in idealized O_h symmetry as follows: 8000−9000 cm^{-1}, $^3A_{2g}(F)$ to $^3T_{2g}(F)$; 16 100 cm^{-1}, $^3A_{2g}(F)$ to $^3T_{1g}(F)$; 25 000 cm^{-1}, $^3A_{2g}(F)$ to $^3T_{1g}(P)$. The transitions are shifted to lower wavelengths (higher energies) for the mononuclear Ni(**L2**)·$(NO_3)_2$. Here, the $^3A_{2g}(F)$ to $^3T_{2g}(F)$ transition is seen at 11 100 cm^{-1}, $^3A_{2g}(F)$ to $^3T_{1g}(F)$ appears at 20 000 cm^{-1}, and $^3A_{2g}(F)$ to $^3T_{1g}(P)$ is not seen because it is obscured by other, higher energy transitions.[20] The increased energy is consistent with coordination of the nickel ion in the mononuclear complex to a greater number of strong field ligands. Additionally, the lower intensity for the mononuclear species absorbance bands is due to a ligand field that is closer to O_h symmetry.

Both ligands **L1** and **L2** were designed to be dinucleating. Indeed, **L1** is strictly dinucleating, regardless of the nickel salt used. However, **L2** is dinucleating if $NiCl_2$ is employed but provides a mononuclear complex if $Ni(NO_3)_2$ is used. The likely explanation for this phenomenon is the more labile nature of the nitrate anions combined with the flexibility of the propyl bridge. The chloride anions remain coordinated to the nickel in solution and, therefore, compete with the ligand for coordination sites. Thus, Ni_2(**L2**)Cl_4 is dinuclear. However, nitrate anions dissociate from the nickel in solution, allowing the ligand to wrap around the metal, resulting in a mononuclear complex. This dependence is not seen with **L1** because the phenyl bridge is too rigid to allow all four oximes to easily coordinate to one metal; therefore, **L1** is always dinucleating.

The anion control over nuclearity with ligand **L2** could be either a thermodynamic or a kinetic effect. One possibility is that the mononuclear species is more thermodynamically stable than the dinuclear species and formed preferentially. Alternatively, the dinuclear species could be thermodynamically more stable, with the mononuclear complex preferred by kinetics if the ligand wraps around the first coordinated nickel that is unprotected by NO_3^- anions in a hexadentate manner before a second nickel can coordinate.

When nickel nitrate is used, the resulting complex is always mononuclear, regardless of solvent. That the mononuclear complex is formed rapidly from the dinuclear

(23) Lever, A. B. P. *Inorganic Electronic Spectroscopy*; Elsevier: Amsterdam, 1984.

Scheme 2. Conditions of Formation and Interconversion for the Mononuclear and Dinuclear Complexes of **L2**

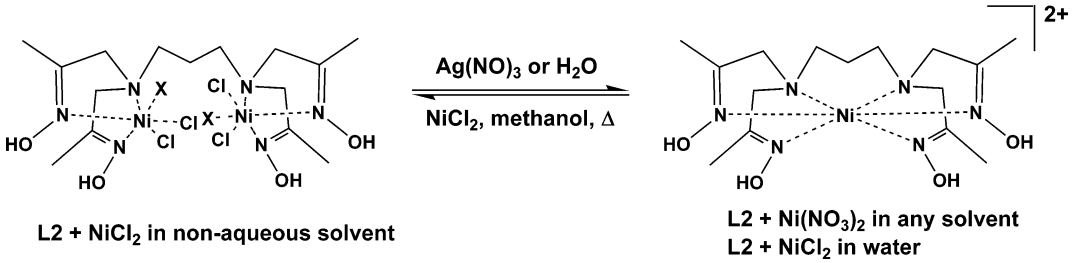

complex when the Cl^-'s are exchanged for NO_3^-'s indicates that the mononuclear species is thermodynamically favored in the absence of coordinating anions. When water is used as the solvent, the mononuclear complex is also preferentially formed. When **L2** and $NiCl_2$ are reacted in water, the dinuclear species is observed transiently but is converted to the mononuclear species over a few seconds. If Ni_2(**L2**)Cl_4 is made in nonaqueous solvent and then dissolved in water, it will spontaneously convert to the mononuclear species (Figure 5). In addition, when excess $NiCl_2$ is added to the mononuclear Ni(**L2**)·$(NO_3)_2$ in water, the complex will not pick up a second nickel (Figure S-4). Thus, in water, the mononuclear species is thermodynamically favored regardless of the counteranion. In the case of strongly coordinating anions (Cl^-) and nonaqueous solvents, the dinuclear species Ni_2(**L2**)Cl_4 is formed; this dinuclear species does not convert to the mononuclear species either over long periods of time (months) or when heated. That the mononuclear complex can be converted into the dinuclear one with the addition of $NiCl_2$ in methanol suggests that the dinuclear complex is thermodynamically preferred when strongly coordinating anions and nonaqueous solvent are present. However, the resulting dinuclear complex is insoluble in nonaqueous solvent; this insolubility may be due to formation of a chloride-bridged polymer of the dinuclear complex rather than the dimer in Figure 2 under the different conditions. An equilibrium between mononuclear Ni(**L2**)·$(NO_3)_2$ and dinuclear Ni_2(**L2**)Cl_4 that favors the mononuclear species cannot be ruled out. In this case, precipitation drives the formation of the dinuclear complex despite an unfavorable equilibrium for that complex. The solvent effect in the thermodynamic preference of mononuclear or dinuclear complexes in the presence of chloride is not due to the coordinating ability of water, since it is not coordinated in the mononuclear complex that is preferred in water. Rather, it is likely due to the greater ability of water relative to nonaqueous solvents to solvate the chloride anions and the Ni(**L2**) dication, stabilizing the mononuclear complex in its equilibrium with the neutral dinuclear complex.

Conclusion

Two new bridged, poly(oxime) ligands and their corresponding nickel complexes have been synthesized. Both ligands coordinate two nickels when the chloride salt is used. However, when the nitrate salt is used, **L1** coordinates two nickels, while **L2** coordinates only one nickel. This difference in binding behavior of the two ligands can be rationalized by the fact that the propyl bridge in **L2** is more flexible than the phenyl bridge in **L1**.

Acknowledgment. Funding was provided by the donors of the Petroleum Research Fund administered by the American Chemical Society (ACS-PRF 37653-AC3) and the University of Cincinnati. Funding for the SMART6000 CCD diffractometer was through NSF-MRI grant CHE-0215950.

Supporting Information Available: Tables of crystallographic data, structure refinement details, atomic coordinates, interatomic distances and angles, anisotropic displacement parameters, and hydrogen parameters in CIF format and figures of UV−vis and IR spectra. This material is available free of charge via the Internet at http://pubs.acs.org.

IC048355X